ACS ES&T Water

pubs.acs.org/estwater

Article

Changes in Molecular Chemistry of Stream Organic Matter and Low Molecular Weight Disinfection Byproduct Precursors Following Initial Post-Fire Rainstorms

William Bahureksa, Charles C. Rhoades, Timothy S. Fegel, Holly K. Roth, Kenneth Hickenbottom, Jacob P. VanderRoest, David Hanigan, Amy M. McKenna, Michael J. Wilkins, and Thomas Borch*

Cite This: https://doi.org/10.1021/acsestwater.6c00583

Read Online

ACCESS | Metrics & More | Article Recommendations | Supporting Information

ABSTRACT: Forested ecosystems are vulnerable to wildfires which have short- and long-term effects on downstream water quality, including changes to dissolved organic carbon (DOC) transport and disinfection byproduct (DBP) formation downstream, which can be exacerbated by high-intensity rainstorms. To evaluate short-term changes to streamwater composition and characteristics, we sampled three streams feeding into the Cache la Poudre River within the perimeter of the 2020 Cameron Peak Fire before, during, and after the first postfire summer storm season. Streams were distinguished by the proportion of their upstream watershed that burned at moderate to high severity (<25%, 25−50%, or >50%). DOC concentration and turbidity demonstrated storm-driven responses that were greatest in the 25−50% burn area stream. Nitrogen-containing species were enriched in streams during the storm and poststorm periods, depending on burn area. Chlorination experiments measured low molecular weight ($C_1 - C_2$) DBPs, where streams from subcatchments with more extensive burns were greater in DOC and DBPs formed across all events. However, DOC released during the storms formed less DBPs on a DOC-normalized basis in all streams. These results demonstrate that DBP formation following wildfire disturbance is primarily driven by storm-mediated increases in DOC loading rather than enrichment in highly reactive pyrogenic material.

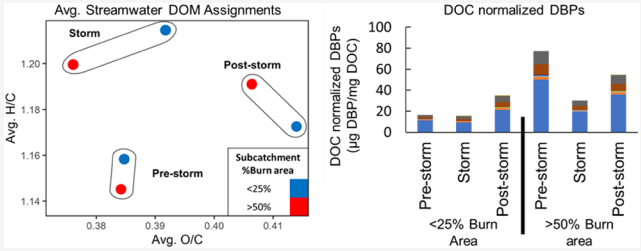

KEYWORDS: *nitrogen, FT-ICR MS, dissolved organic matter, pyrogenic organic matter, disinfection byproducts*

INTRODUCTION

Forest ecosystems in the United States provide numerous ecosystem services (e.g., water resources, soil stabilization and erosion control, climate regulation, and carbon sequestration) valued at ∼ $5 trillion annually and provide drinking water to more than half of the population of the United States.[1] Western United States watersheds provide water to over 180 million people and are currently pressured by population growth and changing climate.[2,3] There are clear links between water quality and forest disturbances, such as wildfires, with projected increases in wildfire size, severity, and frequency likely to have more drastic impacts on aquatic resources and downstream water supply.[4,5] As wildfires continue to grow in frequency and severity, understanding the molecular-level impacts of wildfires on forested watersheds is critical for securing water resources and protecting ecosystem services.

Wildfires directly impact watershed and streamwater quality by burning vegetation and organic soil layers. Litter removal combined with the disruption of soil aggregates postfire greatly exacerbates the transport of ash, char, sediment, and nutrients,[6,7] including dissolved organic matter (DOM) (i.e., dissolved organic carbon (DOC), dissolved organic nitrogen) and total dissolved nitrogen (TDN) from surrounding unburnt and fire-impacted soils and vegetation.[8−10] The degree of combustion of soil and plant organic matter varies widely within wildfires due to spatial heterogeneity in fuel, weather conditions, and site topography; therefore, variation in fire behavior generates a mixture of unburnt, partially charred, and thoroughly charred organic matter. Charring and incomplete combustion of organic matter produces a complex and polyfunctional mixture referred to as pyrogenic organic matter (pyOM), which can retain features from the original organic matter source while exhibiting increased oxidation, acidity, and aromaticity in a continuum.[11−13] The quantity and composition of pyOM formed depends on specific watershed features (e.g., soil profile, soil moisture, topography, vegetation,

Received: April 21, 2026
Revised: August 11, 2026
Accepted: August 12, 2026

© XXXX American Chemical Society

microbial communities)[14−17] and burn severity, defined as the amount of vegetation and litter consumed.[18]

Physical and chemical features can change in streamwater shortly after a fire,[19,20] often in response to precipitation events. Soil heating and pyOM formation generates hydrophobic layers in soils that decrease postfire infiltration and increase erosion and runoff into streams.[14] Stream water is strongly influenced by the presence, intensity, and proximity of a stream to storm events.[21,22] During proximal storm events, nitrate, manganese, total suspended solids, chloride, and DOC concentration can increase by orders of magnitude downstream from burned watersheds.[9,21,23] Various N forms (i.e., nitrate, ammonium, and dissolved organic nitrogen) have also been observed to increase in the years after forest fires in western North American forests, with these trends attributed to postfire summer storms.[24−26] Stream water DOM composition can also shift between storm onset and peak discharge;[27,28] one study found that increased DOM concentration correlated more strongly with watershed discharge than with burn extent.[29] Unique contributions to stream DOM composition can also be introduced via rain-derived DOM,[30,31] though quantifying each contribution was outside the scope of the current study. Thus, storm events are critical in shaping streamwater quality and DOM concentration and composition after wildfires, with their impacts varying by specific watershed characteristics and storm dynamics.

Wildfire-induced transformation of streamwater composition can adversely impact downstream water treatment particularly with disinfection byproduct formation. Disinfection byproducts (DBPs) formed through chlorination treatment of DOC are highly toxic and regulated by the United States Environmental Protection Agency (US EPA).[32] Wildfire-impacted waters have been shown to contain higher DBP formation potential compared to water associated with unburned areas,[33] and can increase further after precipitation events.[34,35] Evaluation of Colorado streams impacted by the 2002 Hayman Fire revealed that increased DBP formation potential correlated to burn severity and DOC concentration.[36] A recent study of California streams affected by the 2021 Caldor Fire and the 2022 Mosquito Fire suggests that burned watersheds experience prolonged releases of DOC and increased DBP formation during storm events compared to unburned areas.[35] Additionally, the speciation and composition of the majority of aromatic DBPs and DBP precursors formed during forest wildfires remains limited due to molecular complexity, polyfunctionality, and heterogeneity of DOM that challenges most routine analytical techniques for molecular identification and quantification.[37,38] Indeed, a recent study reported a positive correlation between highly aromatic and oxidized residues and DBP formation (i.e., trihalomethane and haloacetonitrile) in surface and groundwater.[39] However, little is known about molecular-level compositional changes that transform in-stream DOM and DBP precursors throughout watershed catchments relative to percent burn area and precipitation.

Molecular speciation of DOM compounds in highly complex surface water samples is already challenged by the molecular complexity inherent in DOM; however, DOM pools in postfire watersheds are even more diverse and compositionally complex thereby requiring even higher resolving power mass accuracy. Only Fourier transform ion cyclotron resonance mass spectrometry at 21 T (21 T FT-ICR MS) routinely achieves ultrahigh mass resolving power across a wide molecular weight range and subpart-per-million mass measurement accuracy that enables resolution and subsequent elemental composition assignment to tens of thousands of species in soil and dissolved organic matter.[13,40−45] The ability to routinely achieve resolving power in excess of 3,000,000 at m/z 200 makes FT-ICR MS ideal for analyzing complex environmental samples (e.g., DOM,[46−60] solid and water-soluble char residues,[61−69]), where isobaric species can differ by roughly the mass of an electron.[45,70] Electrospray ionization, which selectively ionizes polar organic species, combined with 21 T FT-ICR MS analysis of forest soil organic compounds, have shown the leaching and degradation of charcoal-derived condensed aromatic species in surrounding pore and stream waters.[71,72] Therefore, FT-ICR MS provides the highest capability in identifying changes to composition across tens of thousands of unique molecules in complex environmental mixtures.

We addressed knowledge gaps in the molecular impacts of wildfires on organic matter stream chemistry and disinfection byproduct formation by analyzing storm-derived changes to DOM composition and DBP formation potential in streams impacted by the largest wildfire in Colorado history: the 2020 Cameron Peak Fire. The Cameron Peak Fire burned 84,544 ha in 2020 within the Cache la Poudre and Big Thompson watersheds which deliver agricultural, municipal and industrial water to more than 300,000 residents in Northern Colorado.[73] Here, we applied electrospray ionization 21 T FT-ICR MS to compare DOM speciation from streams derived from catchments with varying high severity burn area before, during, and after the first Summer storm season after the Cameron Peak Fire. We define this time frame (i.e., within the first year and initial storm season after the end of the fire) as short-term, when char residues and ash are most abundant and least weathered. During this time, precipitation-driven mobilization of fire residues can degrade water quality, alter DOM composition, increase DBP formation potential, and elevate risks of erosion and flooding, with consequences for downstream infrastructure and aquatic ecosystems.

■ MATERIALS AND METHODS

Site Description and Sample Collection

Sampling took place after the Cameron Peak Fire was extinguished (January 2021). A map of the burn area of the Cameron Peak Fire with the watershed area associated with each stream is outlined in Figure S1. Stream water samples were collected in 2021 before, during, and after high intensity summer rainstorms during the first postfire storm season, where measurements were averaged over multiple days that culminate into prestorm, storm, and poststorm sampling periods. Stream water samples were collected from three subcatchments of the Cache la Poudre River Watershed and were classified by the percent of moderate and high severity burn area (BA) in each subcatchment, where burn severity was differentiated using standard remote sensing approaches.[74] Moderate and high severity burns are characterized by the combustion of most vegetation and organic soil layers[18] and typically result in more pronounced short-term changes in watershed streamwater chemistry.[19,75] Samples were collected from streams associated with the following subcatchments: South Lone Pine, (2,226 ha, 24% burned with 14% at moderate/high severity), Bennett (3,726 ha, 70% burned with 38% at moderate/high severity), and Fish (1,312 ha, 86% burned with 57% at moderate/high severity), where stream samples are referred to as <25% BA, 25−50% BA, and >50% BA streamwater samples, respectively. Each stream was sampled over the following days and grouped by sampling period:

https://doi.org/10.1021/acsestwater.6c00583
ACS EST Water XXXX, XXX, XXX−XXX

prestorm (June eighth 2021, June 15th 2021, June 22nd 2021), storm (July 27th 2021, Aug fourth 2021, Aug 11th 2021), and poststorm (Oct 12th 2021, Oct 27th 2021, Dec first 2021) (Figure S2).

Stream Water Chemistry

Stream water samples were collected in plastic sample collection bottles (high density polyethylene) that were triple washed with deionized water (SC < 1.0 μS cm^{-1}). Samples were refrigerated after collection, then aliquots for DOC and TDN were filtered through 0.7 μm mesh glass fiber prefilters (Millipore Corporation, Billerica, MA, USA). Samples were analyzed within 72 h of collection. Both DOC and TDN were determined by high-temperature combustion catalytic oxidation using a Shimadzu TOC-V$_{CPN}$ total organic carbon analyzer with a TNM-1 total nitrogen detection unit (Shimadzu Corporation Columbia, MD, USA). Detection limits for DOC and TDN were 0.05 mg L^{-1}. Turbidity was measured in 1 L samples using the nephelometric method (HF Scientific, Inc. Micro 100 Turbidimeter).[76] Measurements were averaged over sampling periods for water chemistry analysis and compared using single factor ANOVA and Tukey's HSD to determine significant differences between sampling periods of each respective stream ($p < 0.05$, $\alpha < 0.05$) (Table S1).

Twenty-One Tesla Electrospray Ionization Fourier Transform Ion Cyclotron Resonance Mass Spectrometry (21 T FT-ICR MS)

Stream water samples collected on June 15th, Aug fourth, and Oct 27th 2021 were centrifuged for 10 min at 5000 rpm followed by filtering through 0.2 μm poly(ether sulfone) filters. Samples were then acidified to pH 2 with trace-metal grade HCl and prepared for FT-ICR MS using solid-phase extraction with styrene-divinylbenzene (SDVB) polymer modified with a proprietary nonpolar surface (Bond Elut PPL, Agilent Technologies). This solid-phase extraction cartridge was used to capture less polar organic matter residues while removing polar inorganic salts.[40] Solid-phase extraction has been applied to water samples ranging from freshwater to brine and produced water, providing a consistent approach for comparative analysis. While reproducibility can be challenging for complex mixtures lacking compound-specific standards, previous studies have shown that PPL sorbents offer reliable and reproducible performance for dissolved organic matter extraction.[46,77,78] Adsorbed organic species were eluted with methanol and carbon normalized based on the DOC of the water (HPLC grade, Sigma-Aldrich Chemical Co., St. Louis, MO) to yield a final concentration of ∼ 50 ppm carbon and then sent to the National High Magnetic Field Laboratory in Tallahassee, Florida.

Extracts were analyzed with a custom-built hybrid linear ion trap FT-ICR mass spectrometer equipped with a 21 T superconducting solenoid magnet and injected via direct infusion.[79,80] Measurement was completed with both positive and negative mode. The number of formulas assigned between positive and negative mode for each sample were roughly comparable and exhibited similar heteroatom class shifts across the burn area gradient with a few distinctions. On average, positive mode assignments were less oxidized and incorporated more nitrogen. In contrast, negative mode included more sulfur-containing heteroatom assignments (i.e., CHOS, CHNOS) that were also more abundant. Data collected using + ESI was the primary focus of this manuscript; previous study has demonstrated the increased ionization efficiency of fire-impacted DOM in + ESI compared to -ESI.[1] Furthermore, CHNO-containing classes have been shown to increase in abundance and speciation (e.g., newly assigned CHN_3O and CHN_4O) substantially compared to CHO-containing classes during laboratory heating, and are more amenable to + ESI.[2] Due to limited sample volumes collected during rapidly changing storm events and ultrahigh-resolution instrument access, a single representative sample from each stream and sampling date was analyzed. This approach is consistent with prior environmental DOM studies employing FT-ICR MS to evaluate spatial and temporal compositional trends,[13,35,81−83] where molecular characterization focuses on comparative differences among samples rather than analytical replication. Description of the ionization conditions and experimental methods can be found in Supporting Information. All FT-ICR MS data files and assigned elemental compositions are publicly available via the Open Science framework at 10.17605/OSF.IO/ATUR8.

Molecular formulas containing carbon (C_{1-100}), hydrogen (H_{1-200}), oxygen (O_{1-30}), nitrogen (N_{1-5}), and sulfur (S_{1-3}) were assigned and visualized with PetroOrg© software.[84] PetroOrg Assignments also included adducts and isotopes with potential formulas including up to Na_{0-1}, $^{13}C_{0-4}$, $^{15}N_{0-2}$, and $^{34}S_{0-2}$, though these isotope assignments were only used to verify their monoisotopic assignments and reduce false-positives and were not included in the figures or tables. Molecular formula assignments with an error >0.4 parts-per-million were discarded, and only heteroatom classes with a combined relative abundance of ≥ 0.15% of the total were considered. Between 6000 and 16,000 peaks were assigned molecular formulas with <30 ppb RMS error across the samples (Table S2). While isotopes were assigned and used to verify peak assignments with fine isotope structure validation, isotopes and sodiated adducts were omitted in the plots, tables, and discussion here. Assigned elemental formulas of neutral species were used to calculate the aromaticity index-adjusted double-bond-equivalents (AI-adjusted DBE, eq 1)[85,86] and modified aromaticity indices (AI_{Mod}, eq 2)[85,86] where C = the number of carbon, O = the number of oxygen, and so on.

$$DBE_{AI} = 1 + C - O - S - \frac{1}{2}(N + P + H) \tag{1}$$

$$AI_{Mod} = \frac{DBE_{AI}}{C - \frac{1}{2}O - N - S} \tag{2}$$

To assess the changes within the organic matter signature across events for a single stream, molecular formulas assigned across events were compared: if the same formula were assigned in every event, this formula was considered "common", whereas assignments made in only one event were considered "unique". Plotting common and unique assignments was accomplished using van Krevelen diagrams which enable rapid visualization of tens of thousands of elemental compositions in a single plot and cataloging of DOM compounds into loose groupings of biogenic precursors based on plots of atomic H/C versus O/C ratios for elemental compositions derived from FT-ICR MS of DOM.[40,87,88] Van Krevelen plot regions were separated based on molecular bonding constraints, where assignments colored as orange and red include aromatic and condensed aromatic moieties in their structures ($AI_{mod} > 0.5$ and $AI_{mod} \geq 0.67$, respectively). Green points indicate plotting above the molecular lability boundary (MLB, H/C ≥ 1.5), established by D'Andrilli,[89] which was approximated after studying trends from DOM across numerous salinity gradients in river, estuary, and ocean waters. While the MLB region does not account for structure or isomers, assignments above the MLB have been correlated as generally more microbially labile. Finally, gray points comprise midsaturated characteristics and lie between the MLB and aromatic plot regions. Midsaturated compounds are defined in this study operationally by their atomic ratios (H/C < 1.5) and calculated aromaticity index ($AI_{mod} < 0.5$). In a practical sense, there may be double bonds in a compound with an $AI_{mod} < 0.5$ that exist outside of rings or with noncarbon heteroatoms. These designations are not all encompassing but have been applied previously and found to be in good agreement in studies with accompanying biological and spectroscopic measurements.[90−92]

Disinfection Byproduct Formation Measurements

The DBP formation potential was evaluated following Uniform Formation Conditions (UFC), as described by Summers et al.[93] Samples were buffered with 1 M borate solution (pH 8 ± 0.2) and chlorinated with 1 M borate-buffered sodium hypochlorite solutions (pH 8 ± 0.2) at 20 ± 1 °C. Preliminary chlorine demand studies were performed with a series of three Cl2:DOC ratios (1.2:1, 1.8:1, and 2.5:1), followed by incubation at room temperature for 24 ± 1 h. A chlorine dose was then selected which yielded a 1 ± 0.4 mg/L Cl_2 residual after 24 h and a 70 mL sample was then dosed accordingly. Ten mL of sample was removed to measure Cl_2 residual after 24 h to confirm a residual of 1 ± 0.4 mg/L Cl_2. Residual chlorine was

https://doi.org/10.1021/acsestwater.6c00583
ACS EST Water XXXX, XXX, XXX−XXX

quenched using 50 μM ascorbic acid and 150 mL of 12 N hydrochloric acid, and the remaining 60 mL of sample was stored for DBP analysis. Storage times were also kept in accordance with EPA methods 552.2 and 551.1 (i.e., maintained at 4 °C in the dark, analyzed within 2 weeks). DBPs were then measured using gas chromatography − electron capture detection (GC-ECD, Agilent 8860). Four trihalomethanes (THMs), six haloacetonitriles (HANs), and four haloacetamides (HAMs) were quantified using a modified EPA method 551.1.[94] Nine haloacetic acids (HAAs) were quantified using EPA method 552.2.

■ RESULTS AND DISCUSSION

Burn Area Drives Changes in Stream Chemistry

Three streams located within the Cameron Peak Fire perimeter were sampled to elucidate changes to water chemistry over 3 days before (prestorm), during (storm), and following (poststorm) high intensity storms during the first summer storm season following the fire. Figure 1 displays the average

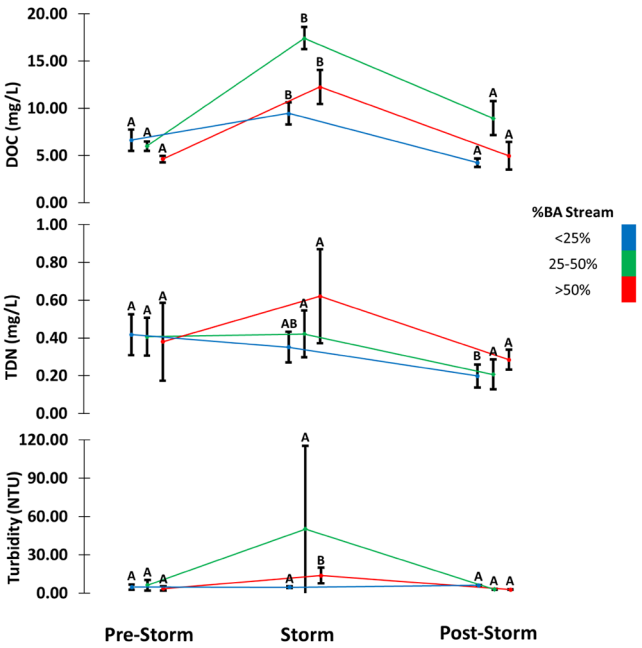

Figure 1. DOC, TDN, and turbidity for each sampling period and stream, colored by burn area (BA) (n = 3). Averages and standard deviations can be found in Table S1. Single factor ANOVA and Tukey's HSD were used to determine significant differences among sampling periods of each respective stream ($p < 0.05$, $\alpha < 0.05$). Significant differences are distinguished by A and B labels.

DOC, TDN, and turbidity of each stream across sampling period (numerical values in Table S1). Recent study has demonstrated the difficulty in differentiating charred and uncharred organic matter due to shared saturation and functional group features.[95−97] Thus, DOC measurements in the current study were considered as including nonimpacted dissolved organic matter and partially charred organic matter, which ranged in impact from light oxidation to near complete combustion.

DOC concentration significantly increased during the storm period and decreased during the poststorm period in each stream (Figure 1). Prestorm DOC was greatest in the <25% BA stream (6.62 mg/L) followed by the 25−50% BA stream (5.99 mg/L) and >50% BA stream (4.61 mg/L). During the storm period, DOC was greatest in the 25−50% BA stream (17.42 mg/L) followed by the >50% BA stream (12.25 mg/L) and <25% BA stream (9.46 mg/L). By the poststorm period, DOC decreased in order the 25−50% BA stream (8.95 mg/L) followed by the >50% BA stream (4.97 mg/L) and <25% BA stream (4.24 mg/L). The 25−50% BA stream exhibited the largest increase in DOC during the storm period, which suggests that a moderate amount of high burn severity area may mobilize more DOC into streams relative to higher or lower amounts. This may be related to increased solubility from partial combustion of DOC without complete oxidation, compared to the <25% BA and >50% BA streams.[98−100] though catchment specific responses may also reflect prefire differences in DOC, topography, and soil properties that are impacted by fine-scale heterogeneity in storm intensity. Regardless, these findings suggest that the amount of subcatchment area burned at high severity will drive changes to stream chemistry and are in agreement with previous findings from the Hayman Fire.[101]

TDN concentrations changed inconsistently from prestorm to storm periods across streams. The average TDN concentrations of each stream were initially similar (0.40 ± 0.02 mg/L) during the prestorm period and displayed unique changes to average TDN concentrations during the storm period: the <25% BA stream decreased (0.35 ± 0.08 mg/L), the 25−50% BA stream stayed relatively the same (0.42 ± 0.12 mg/L), and the >50% BA stream increased (0.62 ± 0.25 mg/L). While the change in average TDN during the storm was not considered significant in the >50% BA stream, the >50% BA stream storm samples included the highest variance and individual measurements among the sampling events. Hydrological and chemical conditions in watersheds can change rapidly during storms and likely contributed to the high variance observed. Despite this, there is evidence that changes in the 25−50% and >50% BA streams may result from the transportation of organic and inorganic nitrogen that can accumulate in ash and be mobilized during storms.[24,102,103] During the poststorm sampling period, the TDN concentration in every stream decreased to below prestorm values, though this decrease was only statistically significant in the <25% BA stream.

Turbidity was similar across streams during the prestorm and poststorm sampling periods and increased during the storm sampling period in the >50% BA stream samples. Turbidity during the storm sampling period was greatest in the 25−50% BA stream (50.17 NTU) followed by the >50% BA stream (13.83 NTU) and <25% BA stream (4.67 NTU). Following the storms, turbidity was not statistically different in any of the streams from prestorm to poststorm sampling periods. Only the >50% BA stream turbidity was significantly higher during the storm period, however the 25−50% BA stream turbidity also exhibited the highest average and variability of the streams. Singular measurements yielding high TDN concentrations contributed to the overall average and may result from the nature of high convection storms, where hydrological and chemical conditions in streams can change on the scale of minutes. In agreement with previous work,[26] turbidity generally increased in waters originating from high %BA watershed areas compared to low %BA watersheds during a precipitation event. The intrastream variability in turbidity was also minimized during the poststorm sampling period, which may be indicative of mixing or the removal of ash and particulate during heavy rainfall that increases heterogeneity of streamwater constituents, though erosion

https://doi.org/10.1021/acsestwater.6c00583
ACS EST Water XXXX, XXX, XXX−XXX

can vary substantially within fire-affected and unburnt watersheds.[9,26]

21 T FT-ICR MS Reveals Unique Nitrogen Speciation in Storm DOM

Unique CHO and CHNO species derived from positive-ion ESI FT-ICR MS were visualized in Van Krevelen plots to disentangle DOM compositional transformations during each sampling period for the <25% and >50% BA stream samples (Figure 2). The percent relative abundance (% R.A.) was calculated only using the CHO and CHNO assignments (Table S2), whereas sulfur-containing heteroatom classes (i.e., CHOS, CHNOS) were <0.1% R.A. of the positive-ion ESI FT-ICR mass spectra and were omitted from this discussion. Analogous diagrams for the 25−50% BA stream can be found in Figure S6.

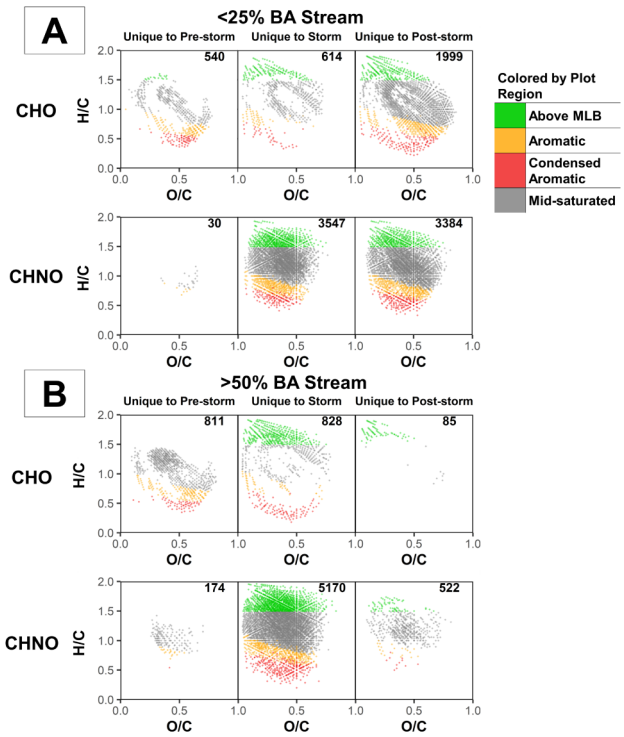

Figure 2. Van Krevelen plots of the unique CHO and CHNO species measured in positive-ion ESI FT-ICR MS for <25% BA stream and >50% BA stream burn area streams across each sampling period. Assignments were considered "unique" if they were not assigned in the prestorm sample spectra (unique formulas in the prestorm were absent from storm and poststorm). Points are colored based on their compositions where assignments colored as orange and red correspond with aromatic and condensed aromatic (CA) moieties in their structures (AI_{mod} > 0.5 and AI_{mod} ≥ 0.67), respectively.[85] Green points indicate the assignments above the molecular lability boundary (MLB, H/C ≥ 1.5)[89] that corresponds with more labile residues, and gray points lie outside these boundaries. Number of assignments per plot region can be found in Table S3. Analogous diagrams for the 25−50% BA stream can be found in Figure S6.

For all samples, DOM mass spectra span mass-to-charge (m/z) 150 − 1000 with an achieved resolving power >2,000,000 at m/z 400 (m/Δm50%, where Δm50% = mass spectral peak width at half-maximum peak height) (Figure S3).[45] Each of the stream samples exhibited a common background DOM signature, which is often reflective of common stream inputs,[63,104,105] that can be seen in the shared compositional space by the molecular formula assignments common to each stream and sampling period (Figure S4). These assignments are indicative of plant and microbial residues that are common to many locations around the South and Midwest United States.[63,104,105] Venn diagrams (Figure S5) also depict the number of shared molecular formulas to show how these assignments overlap among specific sampling events and sites. The following discussion focuses on molecular formula assignments that were unique to each sampling period relative to their respective prestorm samples.

During the storm period, mobilized DOM contained a higher relative abundance of unique nitrogen species compared to prestorm stream samples. DOM in prestorm samples was primarily comprised of CHO species (65%, 56%, and 57% of the total assignments in the <25% BA, 25−50% BA, and >50% BA streams, respectively) followed by CHNO species (34%, 43%, and 42% of the total assignments in the <25% BA, 25−50% BA, and >50% BA streams, respectively). Plotting atomic ratios (H/C vs O/C) of prestorm DOM species reveal the most abundant compositions from midsaturated > aromatic > MLB > condensed aromatic. During the storm period, the CHNO assignments increased and accounted for ∼ 55−60% of the total assignments and ∼ 32% relative abundance while the total number of assignments remained relatively unchanged. Abundances of unique CHNO species in each stream based on atomic ratios ordered from midsaturated > MLB > aromatic > condensed aromatic. Concurrent with an increase in DOC during the storm period, microbially labile nitrogen-containing species in streams are released across all streams during the storm period. Interestingly, the number of CHNO species with multiple nitrogen atoms ($N_{2-4}O_x$) increased in every stream during the storm period and can be rapidly visualized by separating the CHNO heteroatom class by nitrogen content (Figure S7). From the storm to poststorm sampling period, these $N_{2-4}O_x$ assignments only remained enriched in the <25% BA stream whereas the other stream samples resembled their respective prestorm class assignments.

The poststorm DOM composition in the <25% BA stream exhibited unique features to the prestorm DOM and provides insight into how a storm event can impact stream DOM composition in the months following the end of a storm season. By the poststorm period, the CHO and CHNO assignments decreased in every stream to prestorm values except the <25% BA stream where unique CHNO assignments remained high in assignments and % R.A. (from 3547 to 3384 assignments and 19% to 13%). The <25% BA stream poststorm assignments encompassed a larger compositional space compared to the other streams of greater burn area, of which 2550 of the unique poststorm CHNO assignments (compared to prestorm assignments) were also assigned in the storm period. Furthermore, the <25% BA stream featured the greatest number of total and unique assignments in the MLB plot region by the poststorm period. Even after the DOM quantity returned to prestorm conditions (indicated by DOC concentrations), the DOM composition remained altered and enriched with unique nitrogen-containing compounds that appeared microbially labile compared to greater BA streams.

Relative to the prestorm samples, the relative abundance-weighted average molecular weight decreased during the storm (Table S2). During the storm period, average molecular weight of the stream DOM decreased most in the 25−50% BA stream (−53.5 Da), followed by the >50% BA stream (−34.3 Da) and

https://doi.org/10.1021/acsestwater.6c00583
ACS EST Water XXXX, XXX, XXX−XXX

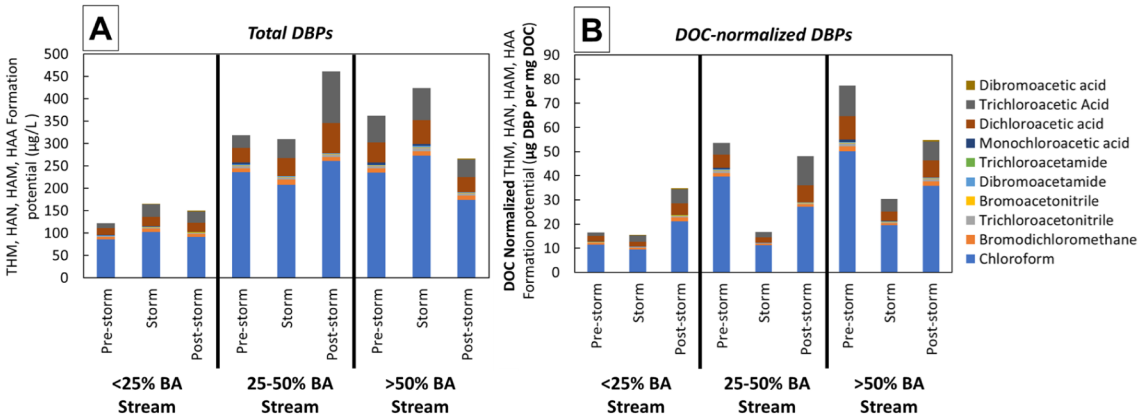

Figure 3. Concentration of disinfection byproducts (DBPs) for each stream through each sampling period after chlorination. A: total DBP concentration. B: DOC-normalized DBP concentration. Values for both total (Table S4) and DOC-normalized (Table S5) DBPs measured in each sample can be found in the Supporting Information. DBPs measured but not shown were below the detection limits.

<25% BA stream (−3.1 Da). The increased abundance of species that contributed to the lower average molecular weight during the storm period corresponded with unique peaks in the MLB plot region and may resemble a rapidly turned-over metabolite fraction released from soil microbial biomass or a lysed fraction of soil microbes that would leach necromass.[55]

Overall, even after the DOM quantity returned to prestorm conditions (indicated by DOC concentrations), the DOM composition remained altered and enriched with unique features that indicate a larger presence of microbially labile residues compared to greater BA streams. Additionally, the increased CHNO assignments and relative abundance in the <25% BA stream do not trend with the DOC or TDN measurements, compared to the greater BA streams, and suggest that the increased DOC, TDN, and unique molecular formulas during the storm period in the 25−50% and >50% BA streams may originate from less severely burned areas in each catchment, regardless of BA.

Changes in DOM Reactivity Influence Disinfection Byproduct Formation

Stream water samples were chlorinated and DBPs were measured, including trihalomethanes (THM), haloacetonitriles (HAN), haloacetamides (HAM), and haloacetic acids (HAA), to quantitatively determine how the difference in stream DOM composition during the prestorm, storm, and poststorm sampling periods may influence drinking water quality and the ability of utilities to meet EPA regulatory standards. Figure 3 shows the total concentration of DBPs formed and measured in each streamwater sample (Figure 3A) and normalized to the DOC of each sample (Figure 3B). While experimental replicates are ideal, they are not always feasible in environmental field studies, particularly in dynamic and remote systems such as the mountain tributaries studied here. Instrument error is typically <3%RSD of the total instrument signal during DBP measurement, and propagated error when calculating the ratio for DOC-normalized DBP concentrations is typically <8%RSD (see appendices section 3).[94] Even considering the extrapolated errors, discussions and interpretations of the data below would remain unchanged. Furthermore, the yields measured here are within expected ranges based on other postfire DBP measurements.[106]

DBP formation was greater in streams with greater proportional burn area and matches previous trends;[98] however, changes to the total DBPs across sampling periods were variable. For prestorm, the total DBP formation in the 25−50% and >50% BA streams (319 and 362 μg/L) was nearly ∼ 3 times that of the <25% BA stream (122 μg/L) (Table S4). These differences stayed similar throughout and after the storm period, but each stream individually had a different increasing and decreasing trend across periods. DOC concentrations increased during the storm period in every stream but DBP formation only increased in two of the streams to varying degrees, highlighting that DOC alone is a poor predictor of DBP formation after fire.

Normalizing DBP formation to the DOC demonstrated a relative decrease in the reactivity of DOM introduced during the storm period (i.e., DOC-normalized DBP formation, or yield, were at a minimum during the storm period (Figure 3B)). The stream with the least proportional burn area (<25% BA) decreased the least compared to prestorm levels, specifically highlighting that pyOM mobilized during the storm period tends to be less reactive in forming DBPs. Poststorm DOC-normalized DBP formation returned to near or slightly below prestorm concentrations except in the <25% BA stream, which nearly doubled the prestorm concentration. The return to slightly below prestorm yield in the greater BA streams likely indicates some remaining, low yielding pyOM persisting in the base flow. The increased reactivity in the <25% BA stream could relate to the enrichment of residues unique to this stream discovered in the poststorm DOM mass spectra, and the significant decrease in TDN that is only present between the <25% BA stream pre- and poststorm sampling period. This suggests that non-pyOM was introduced to the <25% BA stream following the storm period and that increases to total DBP formation following storm events at water utilities may result from greater DOC loading as opposed to increased DOC reactivity.

Environmental Implications

Given the variable coverage and precipitation amount that the high intensity convective storms had on each subcatchment studied here, seasonality and storm specific responses throughout the Cache la Poudre River in Colorado may help explain patterns in the streamwater chemistry and DOC composition. Stream discharge through each sampling site was not measured as monitoring small tributaries can be logistically challenging and highly variable, particularly during storm events. However, Rhoades et al. (2025) reports the discharge through the main stem of the Cache la Poudre and water

https://doi.org/10.1021/acsestwater.6c00583
ACS EST Water XXXX, XXX, XXX−XXX

quality parameters for 16 tributaries from 2020 to 2024, including the ones studied here, to characterize tributary solute concentrations following the Cameron Peak Fire. Across postfire subcatchments, overland-flow impacted potassium, phosphate, ammonium, DOC, turbidity, and total suspended sediment. These solutes exhibited reproducible spikes in their concentration during summer storms, particularly in the first two postfire summers (i.e., 2021 and 2022). The maxima of these solute storm spikes correlated with wildfire extent: tributaries containing >50% BA exhibited the highest solute concentrations, and less or unburned catchments showed smaller but similar patterns. Storm pulses in tributaries appeared to propagate downstream to the mainstem CLP concurrently, highlighting a correlation between wildfire extent, storm mobilization, and stream chemistry. Furthermore, the average DOC, TDN, and turbidity along the main stem increased in 2021 postfire relative to 2020 prefire seasonal means and increased during the 2021 postfire storm season by several fold compared to nonstorm conditions of the same year. Thus, the changes to water chemistry and DOC in the sample set of the current study reflect the influences of storms studied throughout the Cache la Poudre River watershed.

The enriched CHNO residues during the storm period were predominately more saturated and less oxidized compared to the prestorm assignments and might be related to biomolecules released during low temperature burning.[107,108] The unique nitrogen assignments could also represent labile microbial residues,[109] where the poststorm increase in unique assignments in the <25% BA stream compared to the other streams might result from microbes that survived the Cameron Peak Fire at lower severities. A more diverse microbial community would produce a wider range of molecules following precipitation compared to the lower diversity of pyrophilous microorganisms that remain in soils after combustion at higher burn severities.[110] Cao et al. (2025)[111] examined the reactivity of water-extractable organic matter originating from burned and unburned soils using water chemistry and metagenomic analyses. Notably, microbial taxa specializing in the degradation of aromatic compounds were enriched in burned soils, suggesting that wildfires will restructure microbial communities and metabolic pathways involved in postfire organic matter turnover. The unique peaks in the <25% BA stream poststorm sample may also reflect surviving plants and microbes "stimulated" by precipitation relative to the higher burn severity streams through a positive feedback loop,[112] though this assumes living plants and microbes as a predominant source. Another possible source is microbial necromass that can contribute unique residues, where partial combustion under less severe burning could leave more abundant necromass residues capable of transport.[113]

Although it is speculative to approximate the amount of pyOM, allochthonous, and autochthonous DOM introduced due to the compositional overlap of DOM sources observed in streams,[40,50,114−116] this study highlights the reduced reactivity of pyOM as DBP precursors, mobilized during a storm season in streams draining fire-affected catchments. The results reaffirm that short-term declines in water quality will differ among watersheds based on the extent that was burned. It should be noted that DBP quantification only included small molecule targets with 1 to 2 carbon atoms. Larger DBPs formed during chlorination were not characterized by may contribute to the broader spectrum of DBPs forming under experimental conditions. Long-term studies could reveal how DBP precursor loading downstream has increased or decreased compared to prefire conditions, where additional efforts by our team focuses on the long-term changes to postfire watershed water chemistry and the reduced reactivity of organic matter postfire.[117] Decreased organic matter reactivity in combination with the increased overall transport of organic matter out of the system through combustion and runoff may potentially result in longer-term decreases in DBP precursor loading after fire.

■ ASSOCIATED CONTENT

Supporting Information

The Supporting Information is available free of charge at https://pubs.acs.org/doi/10.1021/acsestwater.6c00583.

Web site at DOI: Figures and tables detailing the measured water quality parameters and mass spectrometric results. (Section 1) Description of the FT-ICR MS settings and protocol. (Section 2) (PDF)

■ AUTHOR INFORMATION

Corresponding Author

Thomas Borch − *Department of Chemistry, Colorado State University, Fort Collins, Colorado 80523-1872, United States; Department of Soil and Crop Sciences, Colorado State University, Fort Collins, Colorado 80523-1170, United States;* orcid.org/0000-0002-4251-1613; Phone: +1 (970)491-6235; Email: thomas.borch@colostate.edu

Authors

William Bahureksa − *Department of Chemistry, Colorado State University, Fort Collins, Colorado 80523-1872, United States*

Charles C. Rhoades − *US Forest Service, Rocky Mountain Research Station, Fort Collins, Colorado 80526, United States*

Timothy S. Fegel − *US Forest Service, Rocky Mountain Research Station, Fort Collins, Colorado 80526, United States; Department of Soil and Crop Sciences, Colorado State University, Fort Collins, Colorado 80523-1170, United States*

Holly K. Roth − *Department of Soil and Crop Sciences, Colorado State University, Fort Collins, Colorado 80523-1170, United States;* orcid.org/0000-0003-2733-517X

Kenneth Hickenbottom − *Department of Civil and Environmental Engineering, University of Nevada, Reno, Reno, Nevada 89557, United States;* orcid.org/0000-0002-7488-7391

Jacob P. VanderRoest − *Department of Chemistry, Colorado State University, Fort Collins, Colorado 80523-1872, United States*

David Hanigan − *Department of Civil and Environmental Engineering, University of Nevada, Reno, Reno, Nevada 89557, United States;* orcid.org/0000-0002-6947-7611

Amy M. McKenna − *Department of Soil and Crop Sciences, Colorado State University, Fort Collins, Colorado 80523-1170, United States; National High Magnetic Field Laboratory, Florida State University, Tallahassee, Florida 32310-4005, United States;* orcid.org/0000-0001-7213-521X

Michael J. Wilkins − *Department of Soil and Crop Sciences, Colorado State University, Fort Collins, Colorado 80523-1170, United States*

Complete contact information is available at:
https://pubs.acs.org/10.1021/acsestwater.6c00583

Author Contributions

The manuscript was written through contributions of all authors. All authors have given approval to the final version of the manuscript.

Notes

The authors declare no competing financial interest.

■ ACKNOWLEDGMENTS

This research was funded by the National Science Foundation (1512670, 2114868, 2229313, and 2418390) and the USDA National Institute of Food Agriculture through AFRI grant no. 2021-67019-34608. A portion of this work was funded by the National Science Foundation Division of Chemistry and Division of Materials Research through NSF DMR-2128556, and the state of Florida. We specifically thank the US Forest Service, Rocky Mountain Research Station for sample collection and biogeochemical analysis. Any use of trade, firm, or product names is for descriptive purposes only and does not imply endorsement by the U.S. Government.

■ REFERENCES

(1) Apsalyamova, S. O.; Khashir, B. O.; Khuazhev, O. Z.; Tkhagapso, M. B.; Bgane, Y. K. The Economic Value of Forest Ecosystem Services. *J. Environ. Manage. Tour.* **2015**, *6* (2), 117−122.

(2) Furniss, M. J.; Staab, B.; Hazelhurst, S.; Clifton, C. F.; Roby, K. B.; Ilhadrt, B. L.; Larry, E. B.; Todd, A. H.; Reid, L. M.; Hines, S.et al.Water Climate Change, and Forests: Watershed Stewardship for a Changing Climate*Forest Management For Resilience, Adaptation and Watershed Protection*Department of Agriculture, Forest Service, Pacific Northwest Research Station2012June35−145

(3) Coogan, S. C. P.; Robinne, F. N.; Jain, P.; Flannigan, M. D. Scientists' Warning on Wildfire—a Canadian Perspective. *Can. J. For. Res.* **2019**, *49* (9), 1015−1023.

(4) Ruffault, J.; Curt, T.; Moron, V.; Trigo, R. M.; Mouillot, F.; Koutsias, N.; Pimont, F.; Martin-StPaul, N.; Barbero, R.; Dupuy, J. L.; Russo, A.; Belhadj-Khedher, C. Increased Likelihood of Heat-Induced Large Wildfires in the Mediterranean Basin. *Sci. Rep.* **2020**, *10* (1), 1−9.

(5) Williams, A. P.; Livneh, B.; McKinnon, K. A.; Hansen, W. D.; Mankin, J. S.; Cook, B. I.; Smerdon, J. E.; Varuolo-Clarke, A. M.; Bjarke, N. R.; Juang, C. S.; Lettenmaier, D. P. Growing Impact of Wildfire on Western US Water Supply. *Proc. Natl. Acad. Sci. U. S. A.* **2022**, *119* (10), 1−8.

(6) Smith, H. G.; Sheridan, G. J.; Lane, P. N. J.; Nyman, P.; Haydon, S. Wildfire Effects on Water Quality in Forest Catchments: A Review with Implications for Water Supply. *J. Hydrol.* **2011**, *5*, 170−192.

(7) Zhang, Q.; Wang, Y.; Zhang, Y.; Zhang, J.; Hou, F.; He, C.; Shi, Q.; Zhang, G.; Wang, J. Heating-Induced Changes in Content and Molecular Characteristics of Pyrogenic Dissolved Organic Matter across Soil Types. *Environ. Sci. Technol.* **2025**, *59*, 3937.

(8) Writer, J.H.; Mccleskey, R. B.; Murphy, S.F.; Stone, M.; Collins, A.; Thoms, M.*Effects of Wildfire on Source-Water Quality and Aquatic Ecosystems, Colorado Front Range*IAHS-AISH2012354June117−122

(9) Mast, M. A.; Clow, D. W. Effects of 2003 Wildfires on Stream Chemistry in Glacier National Park, Montana. *Hydrol. Processes* **2008**, *22* (26), 5013−5023.

(10) Revchuk, A. D.; Suffet, I. H. Effect of Wildfires on Physicochemical Changes of Watershed Dissolved Organic Matter. *Water Environ. Res.* **2013**, *86* (4), 372−381.

(11) Santín, C.; Doerr, S. H.; Kane, E. S.; Masiello, C. A.; Ohlson, M.; De La Rosa, J. M.; Preston, C. M.; Dittmar, T. Towards a Global Assessment of Pyrogenic Carbon from Vegetation Fires. *Global Change Biol.* **2016**, *22* (1), 76−91.

(12) Pierson, D. N.; Robichaud, P. R.; Rhoades, C. C.; Brown, R. E. Soil Carbon and Nitrogen Eroded after Severe Wildfire and Erosion Mitigation Treatments. *Int. J. Wildland Fire* **2019**, *28* (10), 814.

(13) Roth, H. K.; Borch, T.; Young, R. B.; Bahureksa, W.; Blakney, G. T.; Nelson, A. R.; Wilkins, M. J.; McKenna, A. M. Enhanced Speciation of Pyrogenic Organic Matter from Wildfires Enabled by 21 T FT-ICR Mass Spectrometry. *Anal. Chem.* **2022**, *94* (6), 2973−2980.

(14) González-Pérez, J. A.; González-Vila, F. J.; Almendros, G.; Knicker, H. The Effect of Fire on Soil Organic Matter—a Review. *Environ. Int.* **2004**, *30* (6), 855−870.

(15) Alcañiz, M.; Outeiro, L.; Francos, M.; Úbeda, X. Science of the Total Environment Effects of Prescribed Fires on Soil Properties: A Review. *Sci. Total Environ.* **2018**, *613−614*, 944−957.

(16) Knicker, H. How Does Fire Affect the Nature and Stability of Soil Organic Nitrogen and Carbon? A Review. *Biogeochemistry* **2007**, *85* (1), 91−118.

(17) Cao, X.; Li, S.-A.; Huang, H.; Ma, H. Wildfire Impacts on Molecular Changes of Dissolved Organic Matter during Its Passage through Soil. *Environ. Sci. Technol.* **2024**, *58* (26), 11436−11446.

(18) Keeley, J. E. Fire Intensity, Fire Severity and Burn Severity: A Brief Review and Suggested Usage. *Int. J. Wildland Fire* **2009**, *18*, 116−126.

(19) Lopez, A. M.; Avila, C. C. E.; VanderRoest, J. P.; Roth, H. K.; Fendorf, S.; Borch, T. Molecular Insights and Impacts of Wildfire-Induced Soil Chemical Changes. *Nat. Rev. Earth Environ.* **2024**, *5* (6), 431−446.

(20) Rodríguez-Cardona, B. M.; Coble, A. A.; Wymore, A. S.; Kolosov, R.; Podgorski, D. C.; Zito, P.; Spencer, R. G. M.; Prokushkin, A. S.; McDowell, W. H. Wildfires Lead to Decreased Carbon and Increased Nitrogen Concentrations in Upland Arctic Streams. *Sci. Rep.* **2020**, *10* (1), 8722.

(21) Murphy, S. F.; Writer, J. H.; McCleskey, R. B.; Martin, D. A. The Role of Precipitation Type, Intensity, and Spatial Distribution in Source Water Quality after Wildfire. *Environ. Res. Lett.* **2015**, *10* (8), 084007.

(22) Moody, J. A.; Martin, D. A. Post-Fire Rainfall Intensity-Peak Discharge Relations for Three Mountainous Watersheds in the Western USA. *Hydrol. Processes* **2001**, *15* (15), 2981−2993.

(23) Greenbaum, N.; Wittenberg, L.; Malkinson, D.; Inbar, M. Hydrological and Sedimentological Changes Following the 2010-Forest Fire in the Nahal Oren Basin, Mt. Carmel Israel−a Comparison to Pre-Fire Natural Rates. *Catena* **2021**, *196*, 104891.

(24) Mast, M. A.; Murphy, S. F.; Clow, D. W.; Penn, C. A.; Sexstone, G. A. Water-Quality Response to a High-Elevation Wildfire in the Colorado Front Range. *Hydrol. Processes* **2016**, *30* (12), 1811−1823.

(25) Uzun, H.; Dahlgren, R. A.; Olivares, C.; Erdem, C. U.; Karanfil, T.; Chow, A. T. Two Years of Post-Wildfire Impacts on Dissolved Organic Matter, Nitrogen, and Precursors of Disinfection by-Products in California Stream Waters. *Water Res.* **2020**, *181*, 115891.

(26) Rhoades, C. C.; Entwistle, D.; Butler, D. The Influence of Wildfire Extent and Severity on Streamwater Chemistry, Sediment and Temperature Following the Hayman Fire, Colorado. *Int. J. Wildland Fire* **2011**, *20* (3), 430−442.

(27) Wagner, S.; Fair, J. H.; Matt, S.; Hosen, J. D.; Raymond, P.; Saiers, J.; Shanley, J. B.; Dittmar, T.; Stubbins, A. Molecular Hysteresis: Hydrologically Driven Changes in Riverine Dissolved Organic Matter Chemistry During a Storm Event. *J. Geophys. Res.: Biogeosci.* **2019**, *124* (4), 759−774.

(28) Fellman, J. B.; Hood, E.; Behnke, M. I.; Welker, J. M.; Spencer, R. G. M. Stormflows Drive Stream Carbon Concentration, Speciation, and Dissolved Organic Matter Composition in Coastal Temperate Rainforest Watersheds. *J. Geophys. Res.: Biogeosci.* **2020**, *125* (9), 1−18.

(29) Barton, R.; Richardson, C. M.; Pae, E.; Montalvo, M. S.; Redmond, M.; Zimmer, M. A.; Wagner, S. Hydrology Rather than Wildfire Burn Extent, Determines Post-fire Organic and Black Carbon Export from Mountain Rivers in Central Coastal California. *Limnol Oceanogr Lett.* **2024**, *9* (1), 70−80.

(30) Altieri, K. E.; Turpin, B. J.; Seitzinger, S. P. Composition of Dissolved Organic Nitrogen in Continental Precipitation Investigated by Ultra-High Resolution FT-ICR Mass Spectrometry. *Environ. Sci. Technol.* **2009**, *43* (18), 6950−6955.
(31) Altieri, K. E.; Turpin, B. J.; Seitzinger, S. P. Oligomers Organosulfates, and Nitrooxy Organosulfates in Rainwater Identified by Ultra-High Resolution Electrospray Ionization FT-ICR Mass Spectrometry. *Atmos. Chem. Phys.* **2009**, *9* (7), 2533−2542.
(32) U.S. Environmental Protection Agency National Primary Drinking Water Regulations: Stage 2 Disinfectants and Disinfection Byproducts Rule. *Fed. Regist.* **2006**, *71*(2), 388−493
(33) Bladon, K. D.; Emelko, M. B.; Silins, U.; Stone, M. Wildfire and the Future of Water Supply. *Environ. Sci. Technol.* **2014**, *48* (16), 8936−8943.
(34) Hohner, A. K.; Cawley, K.; Oropeza, J.; Summers, R. S.; Rosario-Ortiz, F. L. Drinking Water Treatment Response Following a Colorado Wildfire. *Water Res.* **2016**, *105*, 187−198.
(35) Hickenbottom, K.; Pagilla, K.; Hanigan, D. Wildfire Impact on Disinfection Byproduct Precursor Loading in Mountain Streams and Rivers. *Water Res.* **2023**, *244*, 120474.
(36) Chow, A. T.; Tsai, K.; Fegel, T. S.; Pierson, D. N.; Rhoades, C. C. Lasting Effects of Wildfire on Disinfection By-Product Formation in Forest Catchments. *J. Environ. Qual.* **2019**, *48* (6), 1826−1834.
(37) Gonsior, M.; Schmitt-Kopplin, P.; Stavklint, H.; Richardson, S. D.; Hertkorn, N.; Bastviken, D. Changes in Dissolved Organic Matter during the Treatment Processes of a Drinking Water Plant in Sweden and Formation of Previously Unknown Disinfection Byproducts. *Environ. Sci. Technol.* **2014**, *48* (21), 12714−12722.
(38) Han, J.; Zhang, X.; Jiang, J.; Li, W. How Much of the Total Organic Halogen and Developmental Toxicity of Chlorinated Drinking Water Might Be Attributed to Aromatic Halogenated DBPs? *Environ. Sci. Technol.* **2021**, *55* (9), 5906−5916.
(39) Milstead, R. P.; Remucal, C. K. Molecular-Level Insights into the Formation of Traditional and Novel Halogenated Disinfection Byproducts. *ACS EST Water* **2021**, *1* (8), 1966−1974.
(40) Bahureksa, W.; Tfaily, M. M.; Boiteau, R. M.; Young, R. B.; Logan, M. N.; McKenna, A. M.; Borch, T. Soil Organic Matter Characterization by Fourier Transform Ion Cyclotron Resonance Mass Spectrometry (FTICR MS): A Critical Review of Sample Preparation, Analysis, and Data Interpretation. *Environ. Sci. Technol.* **2021**, *55* (14), 9637−9656.
(41) Cho, Y.; Ahmed, A.; Islam, A.; Kim, S. Developments in FT-ICR Ms Instrumentation, Ionization Techniques, and Data Interpretation Methods for Petroleomics. *Mass Spectrom. Rev.* **2015**, *34* (2), 248−263.
(42) Matilainen, A.; Gjessing, E. T.; Lahtinen, T.; Hed, L.; Bhatnagar, A.; Sillanpää, M. An Overview of the Methods Used in the Characterisation of Natural Organic Matter (NOM) in Relation to Drinking Water Treatment. *Chemosphere* **2011**, *83* (11), 1431−1442.
(43) Nebbioso, A.; Piccolo, A. Molecular Characterization of Dissolved Organic Matter (DOM): A Critical Review. *Anal Bioanal Chem.* **2013**, *405*, 109−124.
(44) Sleighter, R. L.; Hatcher, P. G. The Application of Electrospray Ionization Coupled to Ultrahigh Resolution Mass Spectrometry for the Molecular Characterization of Natural Organic Matter. *J. Mass Spectrom.* **2007**, *42*, 559−574.
(45) Bahureksa, W.; Borch, T.; Young, R. B.; Weisbrod Chad, C. R.; Blakney, G. T.; Mckenna, A. M. Improved Dynamic Range, Resolving Power, and Sensitivity Achievable with FT-ICR Mass Spectrometry at 21 T Reveals the Hidden Complexity of Natural Organic Matter. *Anal. Chem.* **2022**, *94* (32), 11382−11389.
(46) Li, Y.; Harir, M.; Uhl, J.; Kanawati, B.; Lucio, M.; Smirnov, K. S.; Koch, B. P.; Schmitt-Kopplin, P.; Hertkorn, N. How Representative Are Dissolved Organic Matter (DOM) Extracts? A Comprehensive Study of Sorbent Selectivity for DOM Isolation. *Water Res.* **2017**, *116*, 316−323.
(47) Roth, V. N.; Lange, M.; Simon, C.; Hertkorn, N.; Bucher, S.; Goodall, T.; Griffiths, R. I.; Mellado-Vázquez, P. G.; Mommer, L.; Oram, N. J.; Weigelt, A.; Dittmar, T.; Gleixner, G. Persistence of Dissolved Organic Matter Explained by Molecular Changes during Its Passage through Soil. *Nat. Geosci.* **2019**, *12* (9), 755−761.
(48) Li, Y.; Harir, M.; Lucio, M.; Kanawati, B.; Smirnov, K.; Flerus, R.; Koch, B. P.; Schmitt-Kopplin, P.; Hertkorn, N. Proposed Guidelines for Solid Phase Extraction of Suwannee River Dissolved Organic Matter. *Anal. Chem.* **2016**, *88* (13), 6680−6688.
(49) Hertkorn, N.; Harir, M.; Cawley, K. M.; Schmitt-Kopplin, P.; Jaffé, R. Molecular Characterization of Dissolved Organic Matter from Subtropical Wetlands: A Comparative Study through the Analysis of Optical Properties, NMR and FTICR/MS. *Biogeosciences* **2016**, *13* (8), 2257−2277.
(50) Wagner, S.; Riedel, T.; Niggemann, J.; Vähätalo, A. V.; Dittmar, T.; Jaffé, R. Linking the Molecular Signature of Heteroatomic Dissolved Organic Matter to Watershed Characteristics in World Rivers. *Environ. Sci. Technol.* **2015**, *49* (23), 13798−13806.
(51) Kellerman, A. M.; Kothawala, D. N.; Dittmar, T.; Tranvik, L. J. Persistence of Dissolved Organic Matter in Lakes Related to Its Molecular Characteristics. *Nat. Geosci.* **2015**, *8* (6), 454−457.
(52) Riedel, T.; Zark, M.; Vähätalo, A. V.; Niggemann, J.; Spencer, R. G. M.; Hernes, P. J.; Dittmar, T. Molecular Signatures of Biogeochemical Transformations in Dissolved Organic Matter from Ten World Rivers. *Front. Earth Sci.* **2016**, *4* (September), 85.
(53) Fox, P. M.; Nico, P. S.; Tfaily, M. M.; Heckman, K.; Davis, J. A. Characterization of Natural Organic Matter in Low-Carbon Sediments: Extraction and Analytical Approaches. *Org. Geochem.* **2017**, *114* (Supplement C), 12−22.
(54) Ohno, T.; Parr, T. B.; Gruselle, M. C. I.; Fernandez, I. J.; Sleighter, R. L.; Hatcher, P. G. Molecular Composition and Biodegradability of Soil Organic Matter: A Case Study Comparing Two New England Forest Types. *Environ. Sci. Technol.* **2014**, *48* (13), 7229−7236.
(55) Malik, A. A.; Roth, V. N.; Hébert, M.; Tremblay, L.; Dittmar, T.; Gleixner, G. Linking Molecular Size, Composition and Carbon Turnover of Extractable Soil Microbial Compounds. *Soil Biol. Biochem.* **2016**, *100*, 66−73.
(56) Romero, C. M.; Engel, R. E.; D'Andrilli, J.; Chen, C.; Zabinski, C.; Miller, P. R.; Wallander, R. Patterns of Change in Permanganate Oxidizable Soil Organic Matter from Semiarid Drylands Reflected by Absorbance Spectroscopy and Fourier Transform Ion Cyclotron Resonance Mass Spectrometry. *Org. Geochem.* **2018**, *120*, 19−30.
(57) Tfaily, M. M.; Chu, R. K.; Tolić, N.; Roscioli, K. M.; Anderton, C. R.; Paša-Tolić, L.; Robinson, E. W.; Hess, N. J. Advanced Solvent Based Methods for Molecular Characterization of Soil Organic Matter by High-Resolution Mass Spectrometry. *Anal. Chem.* **2015**, *87* (10), 5206−5215.
(58) O'Donnell, J. A.; Aiken, G. R.; Butler, K. D.; Guillemette, F.; Podgorski, D. C.; Spencer, R. G. M. DOM Composition and Transformation in Boreal Forest Soils: The Effects of Temperature and Organic-Horizon Decomposition State. *J. Geophys. Res.: Biogeosci.* **2016**, *121* (10), 2727−2744.
(59) Patel, K. F.; Tejnecký, V.; Ohno, T.; Bailey, V. L.; Sleighter, R. L.; Hatcher, P. G. Reactive Oxygen Species Alter Chemical Composition and Adsorptive Fractionation of Soil-Derived Organic Matter. *Geoderma* **2021**, *384*, 114805.
(60) Gonsior, M.; Zwartjes, M.; Cooper, W. J.; Song, W.; Ishida, K. P.; Tseng, L. Y.; Jeung, M. K.; Rosso, D.; Hertkorn, N.; Schmitt-Kopplin, P. Molecular Characterization of Effluent Organic Matter Identified by Ultrahigh Resolution Mass Spectrometry. *Water Res.* **2011**, *45* (9), 2943−2953.
(61) Podgorski, D. C.; Hamdan, R.; McKenna, A. M.; Nyadong, L.; Rodgers, R. P.; Marshall, A. G.; Cooper, W. T. Characterization of Pyrogenic Black Carbon by Desorption Atmospheric Pressure Photoionization Fourier Transform Ion Cyclotron Resonance Mass Spectrometry. *Anal. Chem.* **2012**, *84* (3), 1281−1287.
(62) Jiménez-Morillo, N. T.; González-Pérez, J. A.; Almendros, G.; De La Rosa, J. M.; Waggoner, D. C.; Jordán, A.; Zavala, L. M.; González-Vila, F. J.; Hatcher, P. G. Ultra-High Resolution Mass

https://doi.org/10.1021/acsestwater.6c00583
ACS EST Water XXXX, XXX, XXX−XXX

Spectrometry of Physical Speciation Patterns of Organic Matter in Fire-Affected Soils. *J. Environ. Manage.* **2018**, *225*, 139−147.
(63) Wagner, S.; Dittmar, T.; Jaffé, R. Molecular Characterization of Dissolved Black Nitrogen via Electrospray Ionization Fourier Transform Ion Cyclotron Resonance Mass Spectrometry. *Org. Geochem.* **2015**, *79*, 21−30.
(64) Smith, C. R.; Sleighter, R. L.; Hatcher, P. G.; Lee, J. W. Molecular Characterization of Inhibiting Biochar Water-Extractable Substances Using Electrospray Ionization Fourier Transform Ion Cyclotron Resonance Mass Spectrometry. *Environ. Sci. Technol.* **2013**, *47* (23), 13294−13302.
(65) Bahureksa, W.; Young, R. B.; McKenna, A. M.; Chen, H.; Thorn, K. A.; Rosario-Ortiz, F. L.; Borch, T. Nitrogen Enrichment during Soil Organic Matter Burning and Molecular Evidence of Maillard Reactions. *Environ. Sci. Technol.* **2022**, *56*, 4597.
(66) Song, J.; Li, M.; Fan, X.; Zou, C.; Zhu, M.; Jiang, B.; Yu, Z.; Jia, W.; Liao, Y.; Peng, P. Molecular Characterization of Water- And Methanol-Soluble Organic Compounds Emitted from Residential Coal Combustion Using Ultrahigh-Resolution Electrospray Ionization Fourier Transform Ion Cyclotron Resonance Mass Spectrometry. *Environ. Sci. Technol.* **2019**, *53* (23), 13607−13617.
(67) Solihat, N. N.; Yustiawati; Kim, S.; Kim, S. Elucidating Molecular Level Impact of Peat Fire on Soil Organic Matter by Laser Desorption Ionization Fourier Transform Ion Cyclotron Resonance Mass Spectrometry. *Anal Bioanal Chem.* **2019**, *411* (27), 7303−7313.
(68) Wozniak, A. S.; Goranov, A. I.; Mitra, S.; Bostick, K. W.; Zimmerman, A. R.; Schlesinger, D. R.; Myneni, S.; Hatcher, P. G. Molecular Heterogeneity in Pyrogenic Dissolved Organic Matter from a Thermal Series of Oak and Grass Chars. *Org. Geochem.* **2020**, *148*, 104065.
(69) Chen, H.; Tsai, K. -P.; Liu, Y.; Tolić, N.; Burton, S. D.; Chu, R.; Karanfil, T.; Chow, A. T. Characterization of Dissolved Organic Matter from Wildfire-Induced Microcystis Aeruginosa Blooms Controlled by Copper Sulfate as Disinfection Byproduct Precursors Using APPI(−) and ESI(−) FT-ICR MS. *Water Res.* **2021**, *189*, 116640.
(70) Marshall, A. G.; Hendrickson, C. L.; Jackson, G. S. Fourier Transform Ion Cyclotron Resonance Mass Spectrometry: A Primer. *Mass Spectrom. Rev.* **1998**, *17*, 1−35.
(71) Hockaday, W. C.; Grannas, A. M.; Kim, S.; Hatcher, P. G. Direct Molecular Evidence for the Degradation and Mobility of Black Carbon in Soils from Ultrahigh-Resolution Mass Spectral Analysis of Dissolved Organic Matter from a Fire-Impacted Forest Soil. *Org. Geochem.* **2006**, *37* (4), 501−510.
(72) Ide, J.; Ohashi, M.; Köster, K.; Berninger, F.; Miura, I.; Makita, N.; Yamase, K.; Palviainen, M.; Pumpanen, J. Molecular Composition of Soil Dissolved Organic Matter in Recently-Burned and Long-Unburned Boreal Forests. *Int. J. Wildland Fire* **2020**, *29* (6), 541−547.
(73) U.S. Forest Service *Cameron Peak Fire*; https://inciweb.nwcg.gov/incident/6964/.
(74) Parsons, A.; Robichaud, P.; Lewis, S. A.; Napper, C. O.*Field Guide for Mapping Post-Fire Soil Burn Severity*USDA Forest Service - General Technical Report2010
(75) Wilson, C.; Kampf, S. K.; Wagenbrenner, J. W.; MacDonald, L. H. Rainfall Thresholds for Post-Fire Runoff and Sediment Delivery from Plot to Watershed Scales. *For. Ecol. Manage.* **2018**, *430*, 346−356.
(76) APHA *Nephelometric Method—2130b. In Standard Methods for the Examination of Water and Wastewater*; American Public Health Association: Washington, D.C, 1998.
(77) Raeke, J.; Lechtenfeld, O. J.; Wagner, M.; Herzsprung, P.; Reemtsma, T. Selectivity of Solid Phase Extraction of Freshwater Dissolved Organic Matter and Its Effect on Ultrahigh Resolution Mass Spectra. *Environ. Sci.* **2016**, *18* (7), 918−927.
(78) Dittmar, T.; Koch, B.; Hertkorn, N.; Kattner, G. A Simple and Efficient Method for the Solid-Phase Extraction of Dissolved Organic Matter (SPE-DOM) from Seawater: SPE-DOM from Seawater. *Limnol Oceanogr Methods* **2008**, *6* (6), 230−235.
(79) Hendrickson, C. L.; Quinn, J. P.; Kaiser, N. K.; Smith, D. F.; Blakney, G. T.; Chen, T.; Marshall, A. G.; Weisbrod, C. R.; Beu, S. C. Tesla Fourier Transform Ion Cyclotron Resonance Mass Spectrometer: A National Resource for Ultrahigh Resolution Mass Analysis. *J. Am. Soc. Mass Spectrom.* **2015**, *26* (9), 1626−1632.
(80) Smith, D. F.; Podgorski, D. C.; Rodgers, R. P.; Blakney, G. T.; Hendrickson, C. L. 21 T FT-ICR Mass Spectrometer for Ultrahigh-Resolution Analysis of Complex Organic Mixtures. *Anal. Chem.* **2018**, *90* (3), 2041−2047.
(81) Young, R.; Avneri-Katz, S.; McKenna, A.; Chen, H.; Bahureksa, W.; Polubesova, T.; Chefetz, B.; Borch, T. Composition-Dependent Sorptive Fractionation of Anthropogenic Dissolved Organic Matter by Fe(III)-Montmorillonite. *Soil Syst.* **2018**, *2* (1), 14.
(82) Bahureksa, W.; Young, R. B.; McKenna, A. M.; Chen, H.; Thorn, K. A.; Rosario-Ortiz, F. L.; Borch, T. Nitrogen Enrichment during Soil Organic Matter Burning and Molecular Evidence of Maillard Reactions. *Environ. Sci. Technol.* **2022**, *56* (7), 4597−4609.
(83) VanderRoest, J. P.; Fowler, J. A.; Rhoades, C. C.; Roth, H. K.; Broeckling, C. D.; Fegel, T. S.; McKenna, A. M.; Bechtold, E. K.; Boot, C. M.; Wilkins, M. J.; Borch, T. Fire Impacts on the Soil Metabolome and Organic Matter Biodegradability. *Environ. Sci. Technol.* **2024**, *58* (9), 4167−4180.
(84) Krajewski, L. C.; Lobodin, V. V.; Johansen, C.; Bartges, T. E.; Maksimova, E. V.; MacDonald, I. R.; Marshall, A. G. Linking Natural Oil Seeps from the Gulf of Mexico to Their Origin by Use of Fourier Transform Ion Cyclotron Resonance Mass Spectrometry. *Environ. Sci. Technol.* **2018**, *52* (3), 1365−1374.
(85) Koch, B. P.; Dittmar, T. From Mass to Structure: An Aromaticity Index for High-Resolution Mass Data of Natural Organic Matter. *Rapid Commun. Mass Spectrom.* **2006**, *20* (5), 926−932.
(86) Koch, B. P.; Dittmar, T. Erratum: From Mass to Structure: An Aromaticity Index for High-Resolution Mass Data of Natural Organic Matter. *Rapid Commun. Mass Spectrom.* **2006**, *20* (1), 250.
(87) Rivas-Ubach, A.; Liu, Y.; Bianchi, T. S.; Tolić, N.; Jansson, C.; Paša-Tolić, L. Moving beyond the van Krevelen Diagram: A New Stoichiometric Approach for Compound Classification in Organisms. *Anal. Chem.* **2018**, *90* (10), 6152−6160.
(88) Kim, S.; Kramer, R. W.; Hatcher, P. G. Graphical Method for Analysis of Ultrahigh-Resolution Broadband Mass Spectra of Natural Organic Matter, the Van Krevelen Diagram. *Anal. Chem.* **2003**, *75* (20), 5336−5344.
(89) D'Andrilli, J.; Cooper, W. T.; Foreman, C. M.; Marshall, A. G. An Ultrahigh-Resolution Mass Spectrometry Index to Estimate Natural Organic Matter Lability. *Rapid Commun. Mass Spectrom.* **2015**, *29* (24), 2385−2401.
(90) Chen, H.; Ersan, M. S.; Tolić, N.; Chu, R. K.; Karanfil, T.; Chow, A. T. Chemical Characterization of Dissolved Organic Matter as Disinfection Byproduct Precursors by UV/Fluorescence and ESI FT-ICR MS after Smoldering Combustion of Leaf Needles and Woody Trunks of Pine (Pinus Jeffreyi). *Water Res.* **2022**, *209*, 117962.
(91) Tfaily, M. M.; Wilson, R. M.; Brewer, H. M.; Chu, R. K.; Heyman, H. M.; Hoyt, D. W.; Kyle, J. E.; Purvine, S. O. Single-Throughput Complementary High-Resolution Analytical Techniques for Characterizing Complex Natural Organic Matter Mixtures. *J. Visual. Exper.* **2019**, No. 143, No. e59035.
(92) McKenna, A. M.; Chacón-Patiño, M. L.; Chen, H.; Blakney, G. T.; Mentink-Vigier, F.; Young, R. B.; Ippolito, J. A.; Borch, T. Expanding the Analytical Window for Biochar Speciation: Molecular Comparison of Solvent Extraction and Water-Soluble Fractions of Biochar by FT-ICR Mass Spectrometry. *Anal. Chem.* **2021**, *93* (46), 15365−15372.
(93) Summers, R. S.; Hooper, S. M.; Shukairy, H. M.; Solarik, G.; Owen, D. Assessing DBP Yield: Uniform Formation Conditions. *J. AWWA* **1996**, *88* (6), 80−93.
(94) Stewart, K.; An, D.; Hanigan, D. Reduction of Haloacetonitrile-Associated Risk by Adjustment of Distribution System pH. *Environ. Sci.: water Res. Technol.* **2023**, *9* (10), 2725−2732.

https://doi.org/10.1021/acsestwater.6c00583
ACS EST Water XXXX, XXX, XXX−XXX

(95) Chang, Z.; Tian, L.; Li, F.; Zhou, Y.; Wu, M.; Steinberg, C. E. W.; Dong, X.; Pan, B.; Xing, B. Benzene Polycarboxylic Acid—A Useful Marker for Condensed Organic Matter, but Not for Only Pyrogenic Black Carbon. *Sci. Total Environ.* **2018**, *626*, 660−667.
(96) Kappenberg, A.; Bläsing, M.; Lehndorff, E.; Amelung, W. Black Carbon Assessment Using Benzene Polycarboxylic Acids: Limitations for Organic-Rich Matrices. *Org. Geochem.* **2016**, *94*, 47−51.
(97) Goranov, A. I.; Chen, H.; Duan, J.; Myneni, S. C. B.; Hatcher, P. G. Potentially Massive and Global Non-Pyrogenic Production of Condensed "Black" Carbon through Biomass Oxidation. *Environ. Sci. Technol.* **2024**, *58* (6), 2750−2761.
(98) Cawley, K. M.; Hohner, A. K.; Podgorski, D. C.; Cooper, W. T.; Korak, J. A.; Rosario-Ortiz, F. L. Molecular and Spectroscopic Characterization of Water Extractable Organic Matter from Thermally Altered Soils Reveal Insight into Disinfection Byproduct Precursors. *Environ. Sci. Technol.* **2017**, *51* (2), 771−779.
(99) Santos, F.; Russell, D.; Berhe, A. A. Thermal Alteration of Water Extractable Organic Matter in Climosequence Soils from the Sierra Nevada, California. *JGR Biogeosci.* **2016**, *121* (11), 2877−2885.
(100) Hohner, A. K.; Rhoades, C. C.; Wilkerson, P.; Rosario-Ortiz, F. L. Wildfires Alter Forest Watersheds and Threaten Drinking Water Quality. *Acc. Chem. Res.* **2019**, *52* (5), 1234−1244.
(101) Chen, H.; Rhoades, C. C.; Chow, A. T. Characteristics of Soil Organic Matter 14 Years after a Wildfire: A Pyrolysis-Gas-Chromatography Mass Spectrometry (Py-GC-MS) Study. *J. Anal. Appl. Pyrolysis.* **2020**, *152*, 104922.
(102) Knicker, H. "Black Nitrogen" - an Important Fraction in Determining the Recalcitrance of Charcoal. *Org. Geochem.* **2010**, *41* (9), 947−950.
(103) Knicker, H.; González-Vila, F. J.; Polvillo, O.; González, J. A.; Almendros, G. Fire-Induced Transformation of C- and N- Forms in Different Organic Soil Fractions from a Dystric Cambisol under a Mediterranean Pine Forest (Pinus Pinaster). *Soil Biol. Biochem.* **2005**, *37* (4), 701−718.
(104) Zark, M.; Dittmar, T. Universal Molecular Structures in Natural Dissolved Organic Matter. *Nat. Commun.* **2018**, *9* (1), 3178.
(105) Wagner, S.; Jaffé, R.; Stubbins, A. Dissolved Black Carbon in Aquatic Ecosystems. *Limnol Oceanogr Lett.* **2018**, *3* (3), 168−185.
(106) Lokesh, S.; Jathan, Y.; Marchand, E. A.; Hanigan, D. Recent Improvements in Understanding the Impacts of Wildfire on Disinfection Byproduct Formation Potential. *Curr. Opinion Environ. Sci. Health* **2026**, *49*, 100700.
(107) Mataix-Solera, J.; Cerdà, A.; Arcenegui, V.; Jordán, A.; Zavala, L. M. Fire Effects on Soil Aggregation: A Review. *Earth Sci. Rev.* **2011**, *109* (1−2), 44−60.
(108) Sharma, R. K.; Wooten, J. B.; Baliga, V. L.; Hajaligol, M. R. Characterization of Chars from Biomass-Derived Materials: Pectin Chars. *Fuel* **2001**, *80* (12), 1825−1836.
(109) Osborne, D. M.; Podgorski, D. C.; Bronk, D. A.; Roberts, Q.; Sipler, R. E.; Austin, D.; Bays, J. S.; Cooper, W. T. Molecular-Level Characterization of Reactive and Refractory Dissolved Natural Organic Nitrogen Compounds by Atmospheric Pressure Photo-ionization Coupled to Fourier Transform Ion Cyclotron Resonance Mass Spectrometry. *Rapid Commun. Mass Spectrom.* **2013**, *27* (8), 851−858.
(110) Nelson, A. R.; Narrowe, A. B.; Rhoades, C. C.; Fegel, T. S.; Daly, R. A.; Roth, H. K.; Chu, R. K.; Amundson, K. K.; Young, R. B.; Steindorff, A. S.; Mondo, S. J.; Grigoriev, I. V.; Salamov, A.; Borch, T.; Wilkins, M. J. Wildfire-Dependent Changes in Soil Microbiome Diversity and Function. *Nat. Microbiol.* **2022**, *7* (9), 1419−1430.
(111) Cao, X.; Ma, H.; Li, S. -A.; Huang, H.; Cui, F.; Tanentzap, A. J. Enhanced Release and Reactivity of Soil Water-Extractable Organic Matter Following Wildfire in a Subtropical Forest. *Environ. Sci. Technol.* **2025**, *59*, 3992−4002.
(112) Belnap, J.; Welter, J. R.; Grimm, N. B.; Barger, N.; Ludwig, J. A. Linkages between Microbial and Hydrologic Processes in Arid and Semiarid Watersheds. *Ecology* **2005**, *86* (2), 298−307.
(113) Bruns, T. D.; Chung, J. A.; Carver, A. A.; Glassman, S. I. A Simple Pyrocosm for Studying Soil Microbial Response to Fire Reveals a Rapid, Massive Response by Pyronema Species. *PLoS One* **2020**, *15* (3), No. e0222691.
(114) Stenson, A. C.; Marshall, A. G.; Cooper, W. T. Exact Masses and Chemical Formulas of Individual Suwannee River Fulvic Acids from Ultrahigh Resolution Electrospray Ionization Fourier Transform Ion Cyclotron Resonance Mass Spectra. *Anal. Chem.* **2003**, *75* (6), 1275−1284.
(115) Ohno, T.; He, Z.; Sleighter, R. L.; Honeycutt, C. W.; Hatcher, P. G. Ultrahigh Resolution Mass Spectrometry and Indicator Species Analysis to Identify Marker Components of Soil- and Plant Biomass-Derived Organic Matter Fractions. *Environ. Sci. Technol.* **2010**, *44* (22), 8594−8600.
(116) Sleighter, R. L.; Hatcher, P. G. Molecular Characterization of Dissolved Organic Matter (DOM) along a River to Ocean Transect of the Lower Chesapeake Bay by Ultrahigh Resolution Electrospray Ionization Fourier Transform Ion Cyclotron Resonance Mass Spectrometry. *Mar. Chem.* **2008**, *110* (3−4), 140−152.
(117) Hickenbottom, K.; Pagilla, K.; Hanigan, D. Wildfire Intensity and Severity Effects on Formation of Disinfection By-Product Precursors in Bench-Scale and Weathered Forest-Scale Soils. *ACS EST Water 6* 4448−4459

https://doi.org/10.1021/acsestwater.6c00583
ACS EST Water XXXX, XXX, XXX−XXX